iJRASET
International Journal For Research in Applied Science and Engineering Technology

INTERNATIONAL JOURNAL FOR RESEARCH

IN APPLIED SCIENCE & ENGINEERING TECHNOLOGY

Volume: 6 **Issue:** IV **Month of publication:** April 2018

DOI: http://doi.org/10.22214/ijraset.2018.4562

www.ijraset.com

Call: 08813907089 | E-mail ID: ijraset@gmail.com

International Journal for Research in Applied Science & Engineering Technology (IJRASET)
ISSN: 2321-9653; IC Value: 45.98; SJ Impact Factor: 6.887
Volume 6 Issue IV, April 2018- Available at www.ijraset.com

Effect of Fe^{3+} in Li-Mn Aluminates synthesized by co-precipitation method for the application of opto-magnetic and Magnetic refrigeration applications

B. Uthayakumar [1], S. Sukandhiya[2], S. Periandy[3], J. Suryakumary[4], R. Roja[5]
[1, 2, 4, 5](Research Scholar, Department of Physics, Kanchi Mamunivar center for PG Studies, Puducherry, India.)
[3](Associate Professor, Department of Physics, Kanchi Mamunivar center for PG Studies, Puducherry, India.)

Abstract: ***The present paper reports physical properties such as structural, optical and magnetic properties of Lithium Manganese Aluminates as parental composition with Fe-ions as dopants, synthesized by co-precipitation method with pH as 10 and bath temperature as 338K. All the prepared samples or sintered in the presence of air at 1173 K. Structural properties of synthesized*** $Li_{1.0}Mn_{0.5}Fe_xAl_{2-x}O_4$ ***(*** $0.0 \leq x \leq 2.0$ ***in steps of 0.5) nano ferrites were carried out with X-ray Diffraction (XRD) and Fourier Transform Infrared Spectroscopy (FTIR). The crystallite size varies non-linearly from 36 to 48 nm. lattice constant decrease with increasing Fe upto x = 1.5. Morphology of samples has been examined using Scanning Electron Microscope (SEM). Components present in composition of are revealed with Energy Dispersive Spectrometer (EDS). Vibrational Sample Magnetometer (VSM) is used to investigate Magnetic parameters: Saturation Magnetization*** M_s***, Remanent Magnetization*** M_r***, Coercivity*** H_c***, Magneto Crystalline Anisotropy K and Magneton Number. Maximum K value and*** M_s ***obtained for x= 2.0***
Keywords: Fe doping, Lithium Manganese Aluminates, Co-Precipitation method, Magnetic parameters, Coercivity

I. INTRODUCTION

The applications of ferrites are growing in leaps and bounds with the advancement in nanotechnology [1]. Recently, nanocrystalline ferrites have attracted the researchers because of their unusual magnetic properties and their potential technological applications. The bulk properties of ferrites changes as its dimensions are changed to nanoscale [2].

Most soft ferrites in practical use have the composition $MOFe_2O_3$ (where M represents a divalent metal ion) and present in spinel system which can present either in one of two structures, the normal spinel can be described as M^{2+} Fe_2^{3+} O_4 and an inverse ferrite as Fe^{3+} (M^{2+}, Fe^{3+}) O_4 [3]. Lithium ferrite and doped lithium ferrites have become much effective materials [4].

There low cost, high saturation magnetization, high curie temperature and hysteresis loop properties make them excellent candidates for high-density recording media, absorbers, and microwave devices [5].

Aluminium has effect great on the electric and magnetic properties of ferrite and have a wide range of applications at radio and microwave frequencies, where electrical and magnetic losses are required to be minimum. As aluminium content increases, the measured magnetic hysteresis curves shows the saturation magnetization and remanent magnetization are decreased [6].

The structural and magnetic properties of ferrites are found to be sensitive to their composition and microstructure, which in turn are dependent on the processing conditions and different synthesis routes [7].

Recently fine particles of spinel ferrites synthesized by wet-chemical methods were shown to have markedly different properties from those prepared by the ceramic method [8].

Several chemical processing techniques are available for the synthesis of ferrites [9-13]. The selection of an appropriate synthetic procedure often depends on the desired properties and the final applications. Among these methods, Chemical co-precipitation was selected as a best method to synthesize nanoparticles.

It is least expensive simplest approach for making nanoparticles, it produce large quantities (order of grams) in relatively short interval of time [14]. P.R.Arjunwadkar et al studied the influence of Al^{3+} on lithium ferrite prepared by chemical method, he reported that increasing Al^{3+} magnetization and the retentivity decreased. and smaller values of coercivity observed it can be attributed to the single domain behavior and suggesting particle sizes less than a critical size. [15].

Present work is to tailor potential novel combination of Lithium Manganese Aluminum nanoferrite and study the structural, optical and magnetic properties of this combination prepared by co-precipitation.

II. MATERIALS AND METHODS

A. Material for synthesis

$Li_1Mn_{0.5}Fe_{2-x}Al_xO_4$ nanoferrites at various concentration of Aluminium ion has been synthesized from Precursors LiCl, $MnCl_2.4H_2O$, $AlCl_3$, $FeCl_3.6H_2O$ and NaOH. Analytical grade of these precursors are purchased from SIGMA ALDRICH, Germany with 98% purity.

B. Synthesis Methodology

A fruitful synthesizing methodology involves correct choice of precursor, its composition and reaction environment. Particularly for wet chemical methods like sol-gel, hydrothermal, co-precipitation and colloid emulsion technique, pH controller plays an important role. For the present work eco friendly NaOH is used to maintain pH. The physio-chemical properties of nanoparticles are greatly influenced by particle size, morphology, purity and chemical composition. Using chemical methods, have been conformed to efficiently control the morphology and chemical composition of prepared nano powder. Among wet chemical techniques sol-gel, hydro thermal and colloid emulsions are time consuming and involve highly unstable alkoxides and difficult to maintain reaction conditions. Co-precipitation is one of the more successful techniques for synthesizing ultrafine nanoparticles having narrow particle size distribution [16].These advantages on co-precipitation method motivated authors to synthesize $Li_1Mn_{0.5}Fe_{2-x}Al_xO_4$ (x = 0, 0.5, 1.5, 2.0) nanoferrites by co-precipitation method. The precursors for Fe ion is taken as 2 M and 1M for other Metals chlorides. They are mixed in stochiometric ratio and added one by one on the basis of their electro-negativity value. Mixture of Aqueous solution is stirred rigorously at 338K for 30 minutes, meanwhile NaOH is added to the brain solution by drop by drop using a burette till solution reaches pH value 10. The required composition of nanoferrites are formed from conversion of metal salt into hydroxide and then transformed into ferrites. The precipitates obtained were thoroughly washed more than three times with double distilled water and acetone. For the present work as synthezied sample and samples sintered at 1173 K are considered for study.

C. Physical measurements

Crystal structure of all the samples were examined by powder X-Ray diffraction XRD patterns at room temperature PANalytical-X'Pert PRO powder diffractometer using Cu-$K_{\alpha 1}$ radiation. Scanning Electron Microscopy (SEM) study was performed by VEGA 3 TESCAN Scanning Electron Microscope, operated at 120 KV. Elemental analysis has been done with BRUKER EDS. Fourier Transform Infrared (FT-IR) spectra were recorded on SHIMADZU FT-IR spectrophotometer using KBr pellets in the range 4000-400 cm^{-1}. The magnetic properties were measured at room temperature by LAKESHORE vibrating sample magnetometer (VSM).

III. RESULT AND DISCUSSION

A. X-Ray Diffraction Analysis

X-ray diffraction pattern of synthesized Fe doped Lithium-Manganese nanospinel Aluminates for the concentration x = 0, 0.5, 1.5 and 2.0 sintered at 1173K are shown in the Fig.1. Major peaks (220), (311), (400), and (440) are present in XRD pattern of all the samples. This matches with $LiFe_2O_4$ JCPDS file.No.88-0671, $MnFe_2O_4$ JCPDS file No.38-0430 [17, 18]. Minor peak (111) present in all sample except x = 0.5 and 1.5, (222) peak present in all samples except x = 1.5 and 2.0. (422) present in all the samples and (620) present in all the samples except. x = 1.5. The Superstructure peak (211), (310), (321) ,(520) and (521) are observed in all concentration, but number superstructure peak appearing in the XRD pattern decreases on increasing Fe dopant. which reveals that Fe dopant influences the composition towards disordered structure. Generally intensity of XRD peaks confirms the crystalline nature of the samples. Addition of Iron with Lithium-Manganese Aluminates increase the crystalline nature of samples it results in increases intensity of XRD peaks. Peaks of XRD pattern shift towards higher diffraction angle, this is due to replacement of smaller ionic radius Al^{3+} ion (r_{Al} = 0.51 Å) by bigger ionic radius Fe^{3+} ion (r_{Fe} = 0.64 Å) in Li-Mn nano Aluminates. Intensity of (220) decreases and (311) increases with increasing Fe content in the sample. Addition of iron ion in the state both Fe^{2+} and Fe^{3+} compensate a stable tetrahedral and octahedral sites distribution. The prominent peaks shift towards higher angle which results in increase of lattice constant. The shift of peaks is in accordance with Bragg's law and substitution of dopant species [19,20]. The intensities of (220) and (440) planes are more sensitive to cations in tetrahedral and octahedral sites respectively [21, 22]. From TABLE 1 it is clear that intensity of (440) decrease with increasing Fe^{3+} and this expressing decreasing Al^{3+} ions in the octahedral sites. Intensity found to reverse for the concentration x = 2 this may be due to absence of Al^{3+} ions in this ratio. Decrease in intensity of (220) peak maybe due to replacement of Fe^{2+}, Fe^{3+} instead of Al^{3+} and migration of Li^{+} ions from octahedral site to tetrahedral site vice versa.

(400), (422), (511), (440) and (620) using Scherer's equation $D = 0.9 \lambda / \beta \cos \theta$, where D is the average crystallite size, β is the full width half maxima, λ is the X-Ray wavelength and θ is the Bragg's angle. Lattice constant has been calculated from equation a = d

$(h^2 + k^2 + l^2)^{1/2}$ Where 'a' is lattice constant, d be the inter planar distance, hkl is miller indices. Lattice strain determined using the Williamson-Hall formula $\varepsilon = \beta / 4 \tan\theta$, Where ε is the lattice strain of the structure. X-ray Density can be calculated by $\rho_x = ZM/Na^3$, Where Z is number of molecules per unit cell, here it is 8. M is Molecular weight of the sample N is Avagadro's Number, 'a' lattice constant. Dislocation density has been found by using the relation $\delta = 15 \varepsilon / a D$, here δ be the dislocation density [23, 24]. All these structural parameters are calculated and tabulated in TABLE 2.

From TABLE 2, The average crystallite size 'D' varying non-linearly by adding higher ionic radius Fe^{3+}ion (r_{Fe} = 0.67 Å) instead of lower ionic radius Al^{3+} ion (r_{Al} = 0.51 Å) and values lies between 36 nm and 48 nm. For x= 0.5 the average crystallite size is less in comparison to x= 0 this may be due to the migration of Mn^{2+} (r_{Mn} = 0.89 Å) to octahedral and Fe^{3+} (r_{Fe} = 0.67 Å)) to tetrahedral sites (A). In nano regime, it is possible that some of Mn^{2+} ions may migrate towards octahedral site. Lattice constant also decreases with incorporation of Fe ion instead of Al ion and their values are 8.2726 Å to 8.2663 Å upto x= 1.5. At x= 2 nonlinearity occur its due to the complete replacement of Al ions by Fe ions. Increase in molecular weight of the $Li_1Mn_{0.5}Al_xFe_{2-x}O_4$ composition and increase in X-Ray density values are due to replacement of higher atomic mass Fe^{3+} (55.84 gm) by lower atomic mass Al^{3+} (26.98 gm). More crystallite size present at x=1.5 having least lattice strain and least dislocation density value.

B. Scanning Electron Microscope (SEM) and Energy Dispersive Spectroscopic (EDS) Analysis

Fig.2 shows the external morphology of $Li_{1.0}Mn_{0.5}Fe_xAl_{2-x}O_4$ nano aluminates samples for the increase in concentration of Fe (x = 0, 0.5, 1.5, 2.0). The micrographs show the agglomerated grain structure with clusters of fine particle clinging together due to presence of Lithium and aluminium in the composition for x = 0, 0.5, 1.5. The morphology is almost uniform and regular having cubic shaped particles at x = 2.0 only. Replacement of Aluminium by Iron manipulated the morphology [25]. Thus results of SEM in agreement with X-Ray diffraction pattern. Disappearance of superstructures result in less agglomerated nature. x=2 having less superstructure and it having less agglomerated surface. The surface of the aluminates samples has a number of fine pores or voids that are attributed to the large amount of Oxygen and chlorine gas liberated during the sintering process. Presence of vacancies results in contraction of Lattice even higher ionic radius dopant is added to the sample [26]. This observation are obtained for x = 0, 0.5, 1.5 except x = 2.0. EDS spectrum for the $Li_{1.0}Mn_{0.5}Fe_xAl_{2-x}O_4$ (x = 0, 0.5, 1.5, 2.0) nano aluminates are recorded with BRUKER EDS and illustrated in Fig.3. This figure shows each peak corresponds to the element added in the prepared nanoferrite which confirmed the presence of elements in respective concentration. Aluminium and iron are the major constituents in the composition. Oxygen, Lithium and Manganese are the next major constituent in the sample. Peak for Lithium is not obtained in EDS spectra because Silicon detector used in Energy Dispersive X-Ray spectroscope for present study is not having sensing ability to detect small amount of energy emitted by very small Lithium ion which is having K shell for auger electron. It is interesting to note that the preparation condition completely favours the formation of mixed ferrite and allow us to study the effect of increasing the Fe content on the properties of the Fe doped Li-Mn nano Aluminates. The peak values variation is due to it stochiometry, for all the concentration. The values of Aluminium vary with the increase in Iron concentration.

C. Fourier Transform Infrared Spectroscopy (FTIR) Analysis

FTIR spectrum of the Fe doped Lithium Manganese Nanoaluminate are shown in Fig.4. Infrared spectroscopy study supported the formation of Fe doped Li Mn Al spinel nano Aluminates with informative of two strong absorption bands around 400 cm^{-1} and 600 cm^{-1} that are common features of all spinel structure [27]. The spinel structure are attributed to the stretching vibrations of the unit cell of the spinel in the tetrahedral (A) site and the metal-oxygen vibration in the octahedral (B) site. These absorption bands are highly sensitive to changes in interaction between oxygen and cations, as well as to the size of the obtained nano-particles [28]. The broadening of the spectral band depends on the statistical distribution of cations over A and B sites. The vibration frequency depends on the cation mass, cation-oxygen distance and bending force [29]. From Fig 4 and Table 3, Intrinsic stretching vibration frequency of metal- oxygen at tetrahedral site observed in a range 666 cm^{-1} - 548 cm^{-1} and its value shifting linearly toward lower frequency with increase in Fe^{3+} concentration. And replacement of Al^{3+} ions by larger atomic mass Fe^{3+} in octahedral sites also results in a decrease (values are 470 cm^{-1} - 407 cm^{-1})in metal oxygen bond length and consequently decrease the wave number of octahedral and tetrahedral sites by increasing substitution content [30,31]. Additional subsidiary peak for tetrahedral is observed at 528.51 cm^{-1} and 505.45 cm^{-1} at 0 and 0.5 concentration respectively. And 483 cm^{-1} for octahedral site. Intensity of the band corresponds to octahedral and tetrahedral site nonlinearly varies when addition Fe ions. It is well known that the intensity ratio is function of change of dipole moment with the internuclear distance. This value represents the contribution of ionic bond Fe-O in the lattice. So the observed increase and decrease in the absorption band intensity with increase in Fe content, is due to perturbation

occurring in Fe-O bonds. The electronic distribution of Fe-O bonds greatly affected by the dopant Fe^{3+} which is having comparatively bigger radius and high atomic weight Al (26.98amu) and Fe (55.84 amu).

D. Vibrational Sample Magnetometer (VSM) Analysis

doped $Li_{1.0}Mn_{0.5}Fe_xAl_{2-x}O_4$ nanoaluminates (x = 0, 0.5, 1.5, 2.0) hysteresis loops are recorded with LAKESHORE Vibrational sample magnetometer at 300 K with applied field as 20 KOe are shown in Fig.5. The value of anisotropy constant was calculated from Stoner-Wohlfarth relation as follows $H_c = K/M_s$ [32] ,Where H_c is the coercivity , M_s saturation magnetization and K magnetic anisotropy constant .Calculation of magnetic moment in bohrmagneton was carried out using the following relation, n_B = (Molecular Weight × M_S)/5585 [33]. Magnetic parameters saturation magnetization (M_s), Remanence Magnetization (M_r), Coercivity (H_c), Squareness ratio, Magnetic anisotropy constant (K) and magneton number are calculated from Hysteresis loop and tabulated in Table 4.Generally magnetic properties in the prepared sample arise from coupling between spin and orbital angular momentum (L-S coupling) and electron spin (S-S coupling) [34]. In the case of spinel nano magnetic ferrite material magnetic parameters are influenced by cation distribution, collinearity and non collinearity (canting) of spins on their surface, crystallite size and dopant. In the present study undoped Li-Mn-Aluminates have hysteresis loop of paramagnetic nature with low M_r value. Doping Fe ions with the composition result in increase in M_r value. For the concentration 1.5 and 2 shows super paramagnetic behavior having M_r value as 15 and 43 emu/g. Maximum magnetization value obtained at x= 2.0 is 97.93 (emu/g). The hysteresis loop shape varies when increasing Fe in the sample and having very low Coercivity value at x= 0.5. Sample which is having more M_s value having high bohr magneton value. The appearance of super-paramagnetic behavior indicates that the sample having magneto crystalline anisotropy, which is important to hold magnetic ions in certain direction, has been overcome by thermal energy [35].

IV. CONCLUSION

Iron doped Lithium Manganese nanoaluminate at various concentration has been successfully synthesized by uncomplicated and cheap co-precipitation method with average crystallite size between 36 nm and 48 nm. Addition of Fe^{3+} ion influenced the structural properties such as Average crystallite size, lattice constant, lattice strain, dislocation density and X-Ray density of the synthesized samples. In SEM, the morphology manipulated by Fe^{3+}ion in the sample and FTIR observation have fine match with results of XRD and SEM. From VSM analysis and Low concentration of Fe^{3+} induced magnetic ordering and crystal disordering. VSM results will be good candidate for opto magnetic applications and magnetic refrigeration.

REFERENCES

[1] A.Pradeep, P.Priyadharsini, G.Chandrasekaran, J.Alloys compds. 509 (2011) 3917
[2] W.A.Bayoumy, M.A.Gabal, J.Alloys compds. 506 (2010) 205
[3] A.Ghasemi, S.Ekhlasi, M.Mousavinia. J.Magn.Magn.Mater 354 (2014) 136-145
[4] S.A. Jadhav J of Magn and Magn Mater 224 (2001) 167
[5] Xiaofei Cao, Kanging Sun, Chang Sun, Liang Leng J. of Magn. Magn. Mater 321 (2009) 2896
[6] A.T. Raghavender, D. Pajic, K. Zadro, T. Milekovic, J of Magn and Magn Mater 316 (2007) 1-7
[7] P.P. Hankare, R.P. Patil, K.M. Garadkar, R.Sasikala, Mater.Res.Bull, 46 (2011) 447
[8] Y.Xuan, Q. Li, G.Yang, J. Magn.Magn.Mater, 312 (2007) 464
[9] J.Giri, T.Sriharsha, D.Bhadur, J.Mater.Chem.14 (2004) 875
[10] M.George, A.M. John, S.S.NAir, P.A. Joy, J.Magn.Magn.Mater.302 (2006) 190
[11] J.Wang, Mater.Sci.Eng. B 127, (2006) 81
[12] P.P.Hankare, V.T.Vader, N.M.Patil, S.D.Jadhav, Mater,Chem,Phys 113 (1) (2009) 233.
[13] S.Z.Zhang, G.L.Messing, J.Am.Cerm. Soc. 73 (1990) 61
[14] H.Shokrollai, Journal of Magn. Magn Mater 320 (3-4) (2008) 463-474
[15] P.R.Arjunwadkar, R.R. Patile, J.Alloys and Compds 611 (2014) 273-277
[16] T.F.Marinca, I.Chicinas, O.Isnard, V.Pop, F.Pop, J.Alloys and compds, 509 (2011) 7931-7936.
[17] G. Aravind J. Magn.Magn.Mater. 378 (2015) 278-284
[18] G. Wang, D.Zhao, Y. Ma, Z.Zhang Applied Surface Sci.428 (2018) 258-263
[19] M.Hashim, S.S.Meena, R.K.Kotnala, S.E.Shirsath, J. of Magn.Magn.Mater, 360 (2014) 21-33
[20] K. Venkateswarlu, M. Sandhyarani, T.A.Nellaiappan, N. Rameshbabu . Procedia Materials Science 5 (2014) 212-221
[21] B.P. Ladgaonkar, A.S. Vaigainkar, Materials Chemistry and Physics 56 (1998) 280-283
[22] C.S.Narasimhan, C.S.Swamy, Physica Status dolidi 59 (1980) 817
[23] B.Uthayakumar, S.Sukandhiya, J.Suryakumary, S.Periandy. IOSR. J of Appl. Phys 9 (5) (2017) 5-12
[24] S.Sukandhiya, B. Uthyakumar, R.Roja, S.Periandy IOSR J. of Appl. Phys 9 (5) (2017) 52-60
[25] S. Rahman, K.Nadeem, M.A.Rehman, M.Mumtaz. Ceram.Int 39 (2013) 5235-5239
[26] S.Prabahar, M.Dhanam, J.Cryst.Growth 41, 1-2 (2005) 285

[27] M. Hashim, S.E.Shirsath, S. Kumar, R. Kumar J. of alloys and compounds 549 (2012) 348-357.
[28] M.Farid, I.Ahmad, S.Aman, S.Kanwal, M.Murtaza, G.Alia Journal of Ovanic research 11 (2015) 1
[29] A.M.Wahba, M.B.Mohammad, Ceramic International 40 (2014) 6127-6135.
[30] A.G.Boshale, B.K.Chougule. Materila Chemistry and Physics 97 (2006) 273
[31] J.Smit, H.P.Jijn, Ferrite (1959)
[32] N.Singh, A.Agarwal, S.Sanghi, P.Singh, Physica B 406 (2011) 687
[33] S.Singhal, K.Chandra, J.Solid State Chem 180 (2007) 296
[34] M.A.Gabbal, Y.M.A.Angari, Materil Chem Physics 118 (2009) 153
[35] A.Verma, T.C.Goel, R.G.Meadiratta, P.Kishan J.Magn.Magn.Mater 208 (2000) 13-19

TABLE 1: Comparison of X-Ray Intensity

Fe content 'x'	Composition	I_{220}	I_{440}
0	$Li_{1.0}$ $Mn_{0.5}Al_2O_4$	100	21.76
0.5	$Li_{1.0}Mn_{0.5}Al_{1.5}Fe_{0.5}O_4$	100	10.86
1.5	$Li_{1.0}Mn_{0.5}Al_{0.5}Fe_{1.5}O_4$	34.26	19.54
2	$Li_{1.0}Mn_{0.5}Fe_2O_4$	100	14.55

TABLE 2: Structural parameters of $Li_{1.0}Mn_{0.5}Fe_xAl_{2-x}O_4$ (x=0.0, 0.5, 1.5, 2.0) sintered at 1173K

Structural Parameter with respect to concentration of dopant Fe (Samples sintered at 1173K)							
Fe content 'x'	Composition	Crystallite Size D (nm)	Lattice Constant a (Å)	Molecular Weight g/mole	X-ray Density g/cm^3	Lattice Strain 10^{-3}	Dislocation Density 10^{15}
0	$Li_{1.0}$ $Mn_{0.5}Al_2O_4$	40.4	8.2726	125.343	2.941191	3.18	1.6144
0.5	$Li_{1.0}Mn_{0.5}Al_{1.5}Fe_{0.5}O_4$	36.4	8.2715	166.756	3.914514	2.751	1.5015
1.5	$Li_{1.0}Mn_{0.5}Al_{0.5}Fe_{1.5}O_4$	47.9	8.2663	195.621	4.600777	2.495	1.4909
2	$Li_{1.0}Mn_{0.5}Fe_2O_4$	36.9	8.4066	210.053	4.696961	3.895	2.0044

ABLE 3: Vibrational frequency of tetrahedral and octahedral sites

Vibrational frequency of tetrahedral and octahedral sites sintered at 1173K					
Fe content 'x'	Composition	$\nu_{1\ tetra}$	$\nu'_{1\ tetra}$	ν'_{2octa}	ν_{2octa}
0	$Li_{1.0}$ $Mn_{0.5}Al_2O_4$	666.22	528.51	-	-
0.5	$Li_{1.0}Mn_{0.5}Al_{1.5}Fe_{0.5}O_4$	624.72	505.45	-	407.1
1.5	$Li_{1.0}Mn_{0.5}Al_{0.5}Fe_{1.5}O_4$	611.23	-	483.54	416
2	$Li_{1.0}Mn_{0.5}Fe_2O_4$	548.5	-	-	470.52

TABLE 4: Magnetic parameters of $Li_{1.0}Mn_{0.5}FeAl_{2-x}O_4$ (x=0.0, 0.5, 1.5, 2.0) sintered at 1173K

Fe content 'x'	Composition	Saturation Magnetization M_s (emu/g)	Remanent Magnetization M_r (emu/g)	Coercivity H_c (Oe)	Mr/Ms	Magneto Crystalline Anisotropy K (erg)	Magneton Number n_B
0	$Li_{1.0}$ $Mn_{0.5}Al_2O_4$	0.6115	0.038	188.8	0.0621	115.45	0.0137
0.5	$Li_{1.0}Mn_{0.5}Al_{1.5}Fe_{0.5}O_4$	3.2703	0.498	122.2	0.1523	399.63	0.0976
1.5	$Li_{1.0}Mn_{0.5}Al_{0.5}Fe_{1.5}O_4$	20.6434	15.36	188.8	0.7441	3897.47	0.7231
2	$Li_{1.0}Mn_{0.5}Fe_2O_4$	97.9373	43.17	166.6	0.4408	16316.35	3.6834

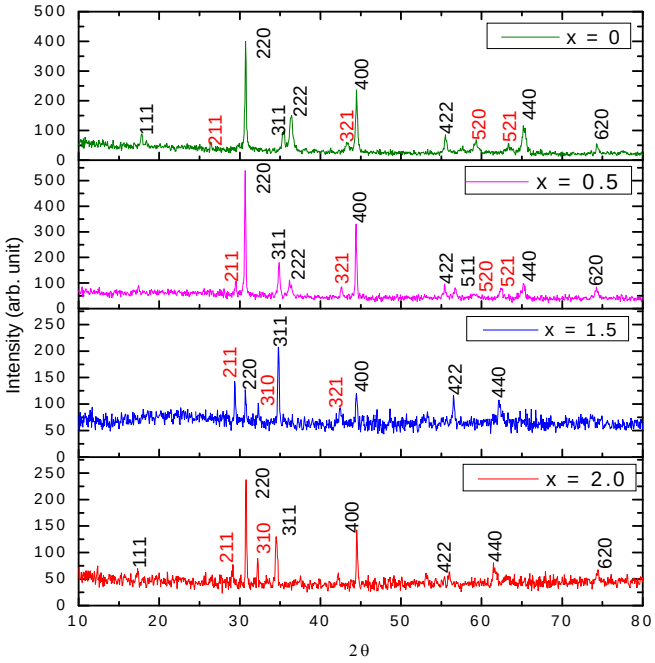

Figure 1: X-Ray Diffraction pattern of $Li_{1.0}Mn_{0.5}Fe_xAl_{2-x}O_4$ (x=0.0, 0.5, 1.5, 2.0) sintered at 1173K

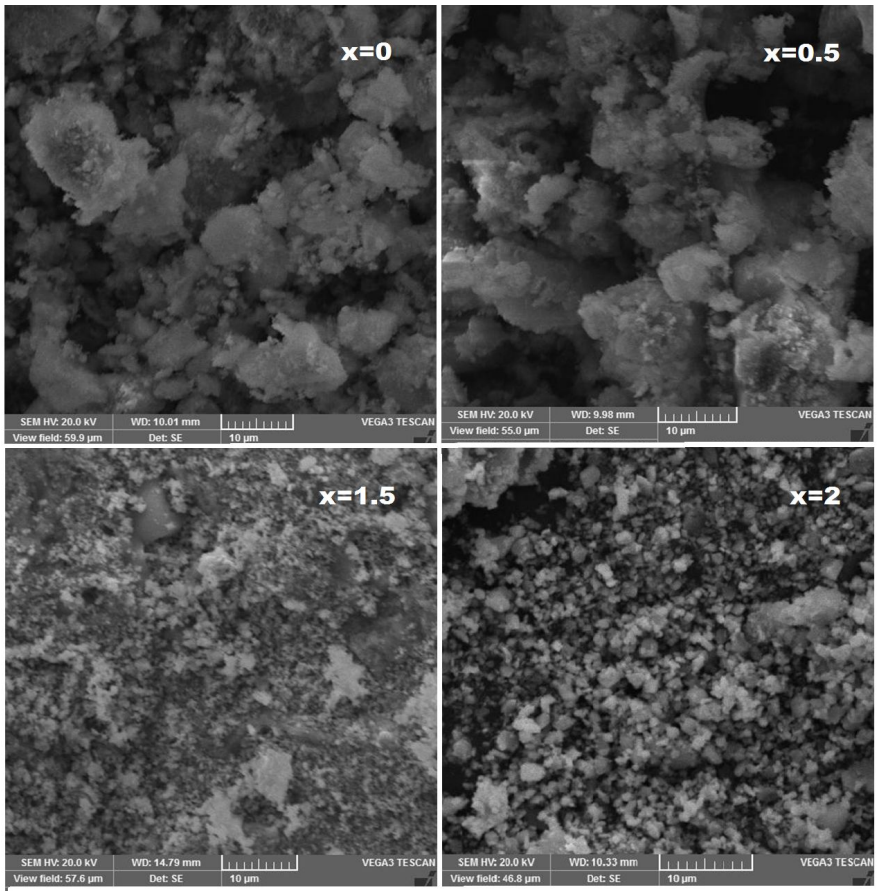

Figure 2. SEM micrograph of $Li_{1.0}Mn_{0.5}Fe_xAl_{2-x}O_4$ (x=0.0, 0.5, 1.5, 2.0) sintered at 1173K

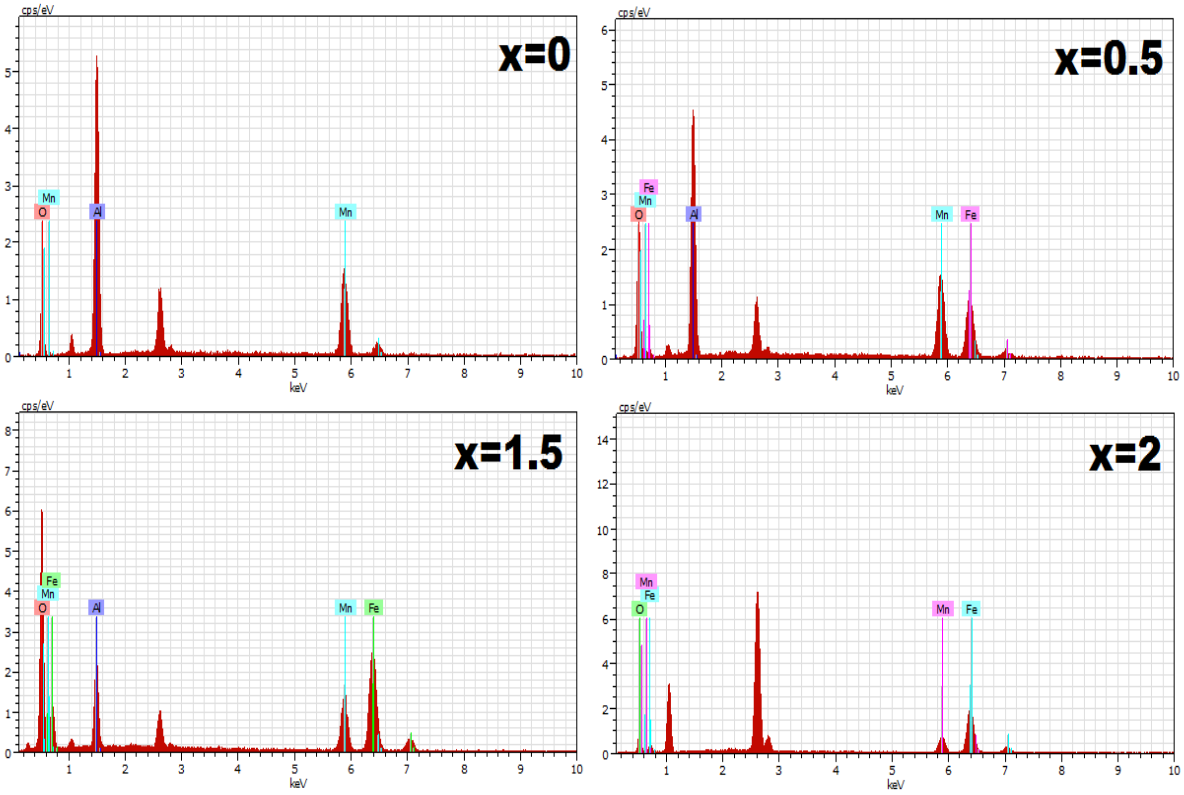

Figure 3: EDS of $Li_{1.0}Mn_{0.5}Fe_xAl_{2-x}O_4$ (x=0.0, 0.5, 1.5, 2.0) sintered at 1173K

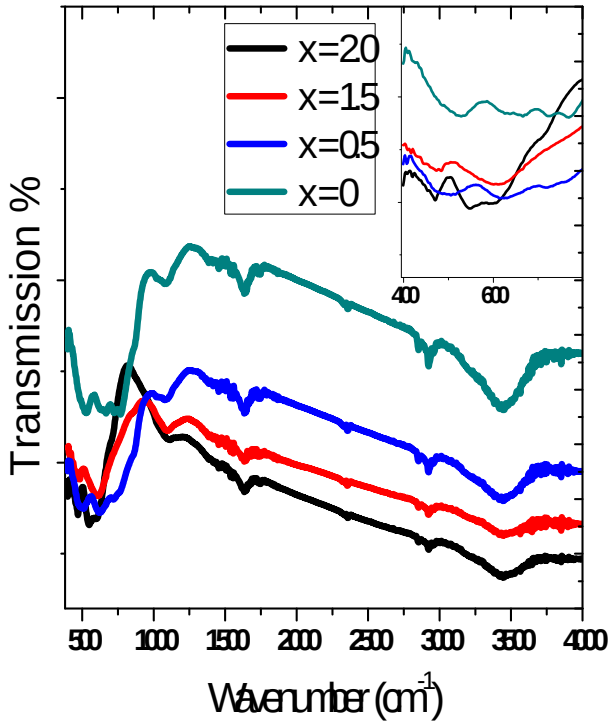

Figure 4: FTIR spectra of $Li_{1.0}Mn_{0.5}Fe_xAl_{2-x}O_4$ (x=0.0, 0.5, 1.5, 2.0) sintered at 1173K

ISSN: 2321-9653; IC Value: 45.98; SJ Impact Factor: 6.887
Volume 6 Issue IV, April 2018- Available at www.ijraset.com

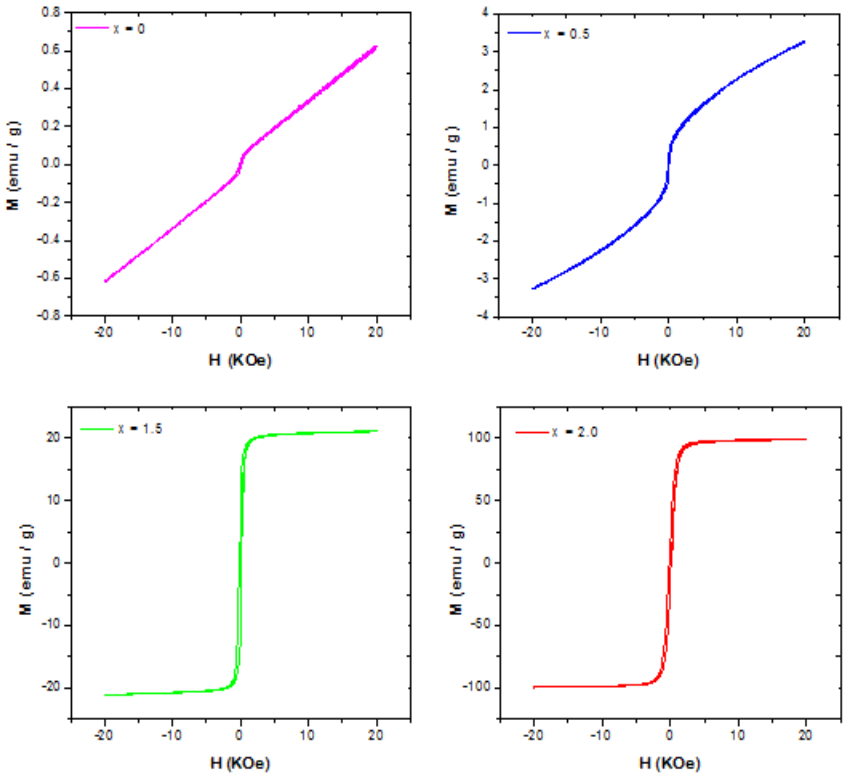

Figure 5: Magnetic hysteresis curves of $Li_{1.0}Mn_{0.5}Fe_xAl_{2-x}O_4$ (x=0.0, 0.5, 1.5, 2.0) sintered at 1173K

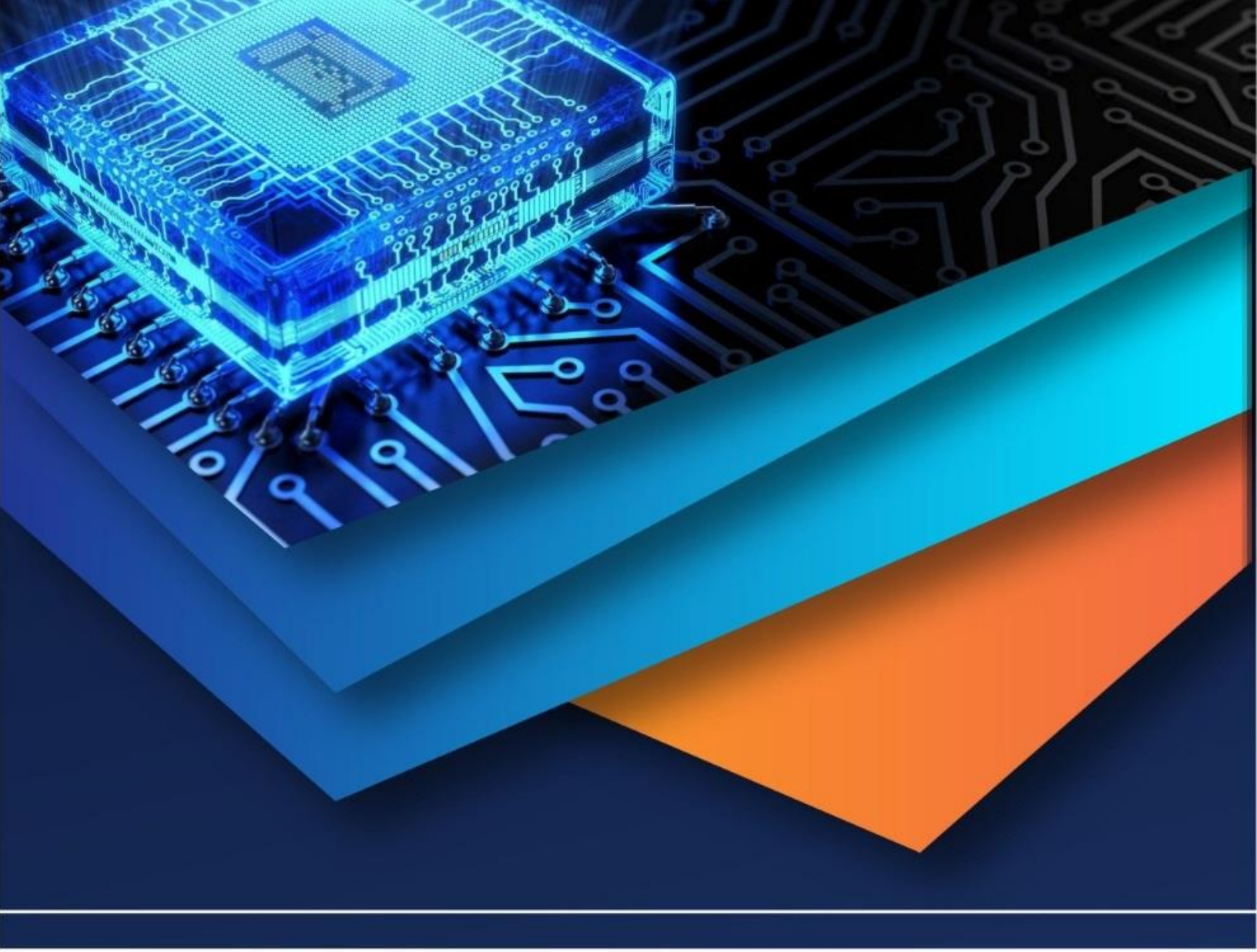

10.22214/IJRASET

45.98

IMPACT FACTOR: 7.129

IMPACT FACTOR: 7.429

INTERNATIONAL JOURNAL FOR RESEARCH

IN APPLIED SCIENCE & ENGINEERING TECHNOLOGY